Resolving the Hydrographic Structure of the Deep Western Boundary Current in the Presence of Topographic Rossby Waves

Robert S. Pickart, WHOI

Numerous moored studies along the continental slope in the mid-Atlantic Bight have revealed that much of the deep variability is due to topographic Rossby waves. These are quasi-geostrophic transverse waves whose flow is nearly along the topography in the low frequency limit. It is believed that the waves are generated offshore by the Gulf Stream, and ultimately propagate onto the continental slope. Possible generation mechanisms include ring-Gulf Stream interactions (Hogg, 1981) and large Gulf Stream meanders (Schultz, 1987).

The SYNOP Inlet Array contained a line of deep current meters across the continental slope off of Cape Hatteras (beneath the surface Gulf Stream). Not surprisingly the observed variability in the 10-50 day band is dominated by topographic Rossby wave motions. The observed dispersion characteristics closely match those predicted by simple theory (Pickart and Watts, 1990). The main purpose of this current meter array, however, was to measure the deep western boundary current (DWBC) which flows equatorward along the continental slope and crosses under the surface Gulf Stream at this location. Speeds in the DWBC are slow compared with those of the superposed topographic waves, and thus at periods up to 50 days it is difficult to detect variations inherent to the

Chlorophyll and Primary Production Distributions in a Gulf Stream Meander

Steven E. Lohrenz, Univ. of So. Mississippi
David A. Phinney, John J. Cullen[1] and
Charles S. Yentsch, Bigelow Laboratory
and Donald B. Olson, RSMAS

Introduction

Mesoscale features of Gulf Stream circulation have been recognized as important in influencing phytoplankton biomass and primary production distributions (e.g. Yentsch, 1974). Numerous studies of Gulf Stream rings have shown close coupling of biomass and production with physical dynamics of the rings (Fryxell et al., 1985; Hitchcock et al., 1985; Nelson et al., 1985; Smith and Baker, 1985; McCarthy and Nevins, 1986; Hitchcock et al., 1987), and ring events provide a mechanism for cross-stream exchange among Slope and Sargasso Sea water species communities (e.g. Ortner et al., 1978; The Ring Group, 1981; Fryxell et al., 1985; Gould and Fryxell, 1988). Other investigations have examined frontal disturbances associated with of the western edge of the Stream which can cause upwelling and intrusion of upwelled water onto the southeastern United States continental shelf (e.g. Atkinson, 1977; Lee et al., 1981). When present, such features are believed to dominate processes affecting primary production on the outer shelf (Yoder et al., 1985).

[1] Present address: Dalhousie Univ., Halifax, Nova Scotia

*   *   *   *   *   *The SYNOP Album!*   *

This is a call for suggestions and figures for the SYNOP album. Several of you have suggested that it would be very useful to bring together a set of figures that would serve as a handy reference in your SYNOP and Gulf Stream work. Obvious ones include bathymetry with all SYNOP instrumentation indicated on it, T/S curves for the region, a cross-section of the current, a spaghetti plot, etc. Please let the editor know what you would like to have included, and feel free to contribute any graphs you think others would find helpful. The figure should be self-explanatory and 'camera ready'. The more eye-catching the better! Our goal is to include the album in the next, year-end issue of the *SYNOPtician.*

boundary current. However, at longer periods (seasonal to inter-annual) the wave energy dies out while the DWBC fluctuations become more energetic, so the array should provide unambiguous information on the DWBC at these relevant time scales.

In summer 1990 a detailed hydrographic survey of the Gulf Stream-DWBC crossover was done. The survey consisted of five sections across the continental slope: two upstream of the crossover, one at the crossover, and two downstream. This experiment was not formally part of SYNOP, but was purposely carried out while the Inlet Array was still in the water so that each experiment would benefit from the other. The hydrographic section at the crossover coincided with the Inlet current meter line. The analysis of the hydrographic data is now underway; the main objective is to determine the manner in which the DWBC crosses under the Gulf Stream. The DWBC is clearly revealed in the property sections (oxygen, silicate, chlorofluorocarbons) which are insensitive to the superposed wave field. However, we are faced with the task of resolving the geostrophic velocity signal of the boundary current in the presence of the topographic waves which are particularly energetic in this region as witnessed by the current meters. This separation can be done for time series data as discussed above (i.e. temporal filtering), but our sections are synoptic realizations which contain both signals. To accomplish this task I employed a spatial filter.

First, relative geostrophic velocity sections were computed using the dynamic method. Next, the sections were converted to absolute velocities by matching the vertically integrated transport between station pairs to absolute velocities by matching the vertically integrated transport between station pairs to acoustic transport float measurements made during the cruise. Figure 1 shows the section of absolute velocity at the Inlet Array line. One immediately notices the bands of alternating equatorward and poleward deep flow located onshore. The current meter data indicate that the dominant waves in this region have wavelength 100-150 km and a vertical scale of 1500-2000 m, which is consistent with this feature.

At first glance one would be tempted to call the equatorward jet between stations 23 and 22 the DWBC; however this jet is too tall and narrow (2000 m high and 50 km wide). The CFC-11 section in Figure 2 suggests that the DWBC (i.e. the deep region greater than 0.3) is instead 150-200 km wide and 1000 m high. I thus employed a spatial filter to remove the high wave number signal, using a 2nd order butterworth filter of width 150 km. This reduces the amplitude of a 100 km wave by 85%, but only reduces a DWBC 150 km wide by 15%. To apply the filter the velocity was interpolated onto a density grid and the filtering was done along density surfaces. In order not to smooth the upper layer Gulf Stream, the filter was only applied below the density surface $\sigma_3 = 40.45$ (dotted line in Figure 1). To avoid a discontinuity at this depth, the width of the filter was initially very small (20 km) and then increased smoothly to a width of 150 km over roughly a 300 m interval.

The resulting filtered velocity is shown in Figure 3, revealing the DWBC core. The high-passed signal which was removed is shown in Figure 4, and as expected the wave signal is strongest onshore. This technique is general and can be applied to any such velocity section across the continental slope (of course for very large topographic wavelengths the separation becomes increasingly difficult). I filtered all five sections and found that only one other section had a significant wave signal; south of the crossover no waves were evident.

References

Hogg, N.G., 1981: Topographic waves along 70°W on the continental rise. Journal of Marine Research, 39, 627-649.

Schultz, J.R., 1987: Structure and propagation of topographic Rossby Waves northeast of Cape Hatteras. M.S. Thesis, Marine Sciences Program, University of North Carolina, 63 pp.

Pickart, R.S. and D.R. Watts, 1990: Deep western boundary current variability at Cape Hatteras. Journal of Marine Research, 48, 765-791.

An aspect of Gulf Stream circulation whose influence on biological parameters is less well studied are meanders occurring offshore east of Cape Hatteras. Meanders, from which rings may develop, are a common circulation feature as the Stream branches eastward from the continental shelf. The physical mechanisms influencing biological distributions within these offshore meanders differ from the topographically constrained frontal disturbances which occur further upstream along the shelf break.

The BIOSYNOP program was an interdisciplinary effort to study biological features of the Gulf Stream front and their response to physical processes associated with meandering of the Gulf Stream (Olson, 1990). Flierl and Davis (1991) presented a model of biological effects of Gulf Stream meandering. Mariano and Hitchcock (1991) and Hitchcock et al. (in prep.) reported strong coherence between pigment fields and physical parameters about the meander, and suggested that mesoscale chlorophyll distributions were controlled by meander physical processes. Preliminary results are presented here describing observed patterns of chlorophyll and primary production in relationship to the physical structure of a meander. We examined the hypotheses that i) different physical regimes within the meander resulted in different photosynthetic properties of the phytoplankton populations, and ii) variability in water column primary production was related to meander physical structure.

Method

Sampling was performed aboard the R/V Cape Hatteras during 21 September - 4 October (Leg 1) and 11-20 October 1988 (Leg 2). Some results from Leg 1 are presented here. Initially, mesoscale surveys were performed consisting of vertical stations transecting the Gulf Stream (Fig. 1A). This was followed by additional sampling at selected locations (Fig. 1B). Positions of stations were guided by AVHRR imagery (Fig. 2) and XBT data. CTD (Seabird) and in situ in

DTIC QUALITY INSPECTED 8

vivo chlorophyll fluorescence (SeaTech) profiles were obtained at all stations. At selected stations, standard fluorometric assays of photosynthetic pigments were performed (Holm-Hansen et al., 1965) and nutrient samples collected. The nutrient samples from the upper mixed layer were preserved and subsequently analyzed on shore by chemiluminescent assay for nitrate + nitrite (Garside, 1982). Deeper samples were frozen, and subsequently analyzed on shore by auto-analyzer (Technicon) following procedures of Whitledge et al. (1981).

Primary Production

At selected stations, primary production was determined generally at six depths throughout the photic zone. Samples were collected using acid-cleaned Niskin bottles with silicon rubber O-rings and cap springs. Subsamples were placed in acid-cleaned 0.25 L polycarbonate bottles, and $NaH_{14}CO^{-3}$ added to a concentration of $0.1 mCi L^{-1}$. Replicate bottles were incubated for 4-6 h and for 24 h under simulated *in situ* conditions in temperature-controlled and spectrally-adjusted deck incubators (Lohrenz et al., 1988, 1991). Zero time and dark bottle samples were also analyzed to account for non-photosynthetic ^{14}C-carbon uptake. ^{14}C activity was quantified as described in Lohrenz et al. (1988). The short term (4-6 h) production rates were normalized to chlorophyll a concentrations and plotted versus the incubation irradiance (Fig. 3). Primary production rates were fit to a non-linear photosynthesis-irradiance equation (Platt et al., 1980):

(1) $P = B * P_S * (1 - \exp(-\alpha * I/P_S)) * (\exp(-\beta * I/P_S))$

where P is the primary production rate (mg C $m^{-3} h^{-1}$), B is biomass concentration (mg chl m^{-3}), P_s is the saturated rate of photosynthesis in the absence of photoinhibition (mg C mg $chl^{-1} h^{-1}$), α is the photosynthetic efficiency (mg C mg chl^{-1} (E $m^{-2})^{-1}$), and β is the photoinhibition constant (mg C mg chl^{-1} (E $m^{-2})^{-1}$). Data were fit using a nonlinear least squares estimation (Systat). The derived P-I parameters were subsequently used to model primary production as discussed below. The photoinhibition parameter was not significantly different from zero for the data presented here and was set equal to zero.

Modelling Pigment and Light Fields

The following empirical relationships for estimating photosynthetic pigments from *in situ* fluorescence ($F_{in\ situ}$) were developed by regression analysis (Leg 1 only):

(2) Chl a + phaeopigments (mg m^{-3}) = $1.17 F_{in\ situ}$ - 0.157

(Model II, $r^2 = 0.68$, N=76)

(3) Chl a (mg m^{-3}) = $0.544 F_{in\ situ}$ - 0.000478 Depth (m) + 0.0922

($r^2 = 0.76$, N = 76)

We compared the relationship given in Eq. 2 with that derived for data from Leg 2 and found them to be similar (Fig. 4).

Continuous measurements of surface irradiance were obtained with a Biospherical Instruments QSR-240 solar reference sensor. Spectral composition of surface irradiance

was approximated using the clear sky irradiance model of Gregg and Carder (1990). *In situ* irradiance was computed from surface irradiance based on a model of vertical attenuation. We used a spectral irradiance attenuation model (Lohrenz et al., 1991) modified from that described by Sathyendranath and Platt (1988). Modifications included omission of angular distribution terms, and use of the expression of Prieur and Sathyendranath (1981) to calculate chlorophyll absorption at 440 nm in place of the expression given by Sathyendranath and Platt (1988). Pigment concentrations were estimated from the empirical relationship with fluorescence (Eq. 2). A 440 nm absorption coefficient for dissolved substances of 0.01 m^{-1} was assumed (cf. Kirk, 1983). The attenuation coefficient for downwelling photosynthetically active radiation (K_{PAR}, m^{-1}) was computed for a given depth interval from the modeled spectral irradiance distribution as follows:

(4) $K_{PAR} = \ln [\int_{400}^{700} I(\lambda, z_{i-1}) d\lambda / \int_{400}^{700} I(\lambda, z_i) d\lambda] / (z_i - z_{i-1})$

where $I(\lambda, z_i)$ is the modeled irradiance at depth z_i. Validation of the model was achieved by direct measurements of K_{PAR} (Li-Cor LI-192SA underwater quantum sensor with LI-192SA surface reference sensor). Modeled and measured K_{PAR} profiles generally agreed well (Fig. 5).

Modeling Primary Production

Vertical profiles of primary production were computed using an approach modified from that of Fee (1973). Production at each depth was estimated from Eq. 1 using the modeled *in situ* irradiance and the chlorophyll concentration estimated from Eq. 3. Depth increments were approximately 5 m and rates were computed at 1 h intervals summed over the photoperiod to give daily production. Total surface irradiance for each interval was scaled to the average determined from measurements during Leg 1 and Leg 2.

Results and Discussion

A comparison of photosynthesis-irradiance relationships for data from different regions within the meander did not reveal significant differences in photosynthetic properties (Fig. 3). Photosynthesis-irradiance data obtained during Leg 2 supported this (cf. Cullen et al., 1991). In the approach presented here, we used a single photosynthesis-irradiance relationship for modeling primary production on the basis of pigment and irradiance distributions (Fig. 3). Modeled estimates of daily production were representative of independent measurements based on 24 h simulated in situ (SIS) incubations (Fig. 6). However, the model tended to underestimate SIS values at low rates and overestimate at high rates. Reasons for underestimation include the fact that the model may not adequately describe increases in photosynthetic efficiency (α) with depth. Reasons for overestimation include the fact that night respiration is not accounted for in the model. It is also possible that the 24 h incubations underestimated production due to effects of containment.

Sections across the core of the Gulf Stream (Fig. 7) show patterns consistent with physical models of meander circulation (e.g. Brooks and Bane, 1983) and independent observations of pigment distributions (Mariano and Hitchcock, 1991; Hitchcock et al., in prep.). In progression from the western (Stations 2-6) to eastern (Stations 20-22) regions of the meander, isopycnal surfaces and the subsurface pigment maximum on Slope Water side of the front deepened. The nitracline showed a similar pattern (data not shown), supporting the view that biomass distributions were influenced by nutrient supply. In the western region on the Slope Water side, the primary production maximum coincided with the subsurface pigment maximum. For the section across the eastern side of the meander, where convergence was expected, a weakening and deepening of the pigment maximum was observed. Furthermore, the production maximum was no longer coincident with the pigment maximum, but instead occurred at St. 3 (0.6 gC m^{-2} d^{-1}) in an area of expected divergence and upwelling of "new" nutrients.

Rates were consistently lower on the Sargasso Sea side of the front (0.4 gC m^{-2} d^{-1} at St. 6 and 22) and intermediate on the Slope Water side in the eastern region (0.5 gC m^{-2} d^{-1} at St. 20).

Conclusions

Our results did not support the hypothesis that different physical regimes within a meander resulted in significant differences in photosynthetic properties of phytoplankton populations. Our use of a single photosynthesis-irradiance relationship to model the primary production distributions yielded results which were representative of direct measurements of daily primary production.

Variability in primary production distributions in the meander could be explained largely on the basis of biomass and irradiance distributions. Biomass distributions presumably reflect a combination of rate processes, including *in situ* growth coupled to nutrient supply, physical transport, and removal by grazers.

Acknowledgements

References

Atkinson L. P. (1977) Modes of Gulf Stream intrusion into South Atlantic Bight shelf waters. Geophys. Res. Letters, 4, 583-586.

Brooks D. A. and J. M. Bane, Jr. (1983) Gulf Stream meanders off North Carolina during winter and summer 1979. J. Geophys. Res., 88, 4633-4650.

Cullen, J. J., X. Yang, H. L. MacIntyre (1991) Nutrient limitation of marine primary productivity. In: Primary Productivity and Biogeochemical Cycles in the Sea, P. G. Falkowski and A. Woodhead (eds.).

Fee, E. J. (1973) Modelling primary production in water bodies: a numerical approach that allows for vertical inhomogeneities. J. Fish. Res. Bd. Can., 30, 1469-1473.

Flierl, G. R. and C. S. Davis (1991) Biological effects of Gulf Stream meandering. Synoptician, 2 (1), 5-7.

Fryxell G. A., R. W. Gould, Jr., E. R. Balmori, and E. C. Theriot (1985) Gulf Stream warm core rings: phytoplankton in two fall rings of different ages. J. Plank. Res., 7, 339-364.

Garside, C. (1982) A chemiluminescent technique for the determination of nanomolar concentrations of nitrate and nitrite in seawater. Mar. Chem., 11, 159-167.

Gould R. W. and G. A. Fryxell (1988) Phytoplankton species composition and abundance in a Gulf Stream warm-core ring. I. Changes over a five month period. J. Mar. Res., 46, 367-398.

Gregg, W. W. and K. L. Carder (1990). A simple spectral solar irradiance model for cloudless maritime atmospheres. Limnol. Oceanogr., 35, 1657-1675.

Hitchcock G., C. Langdon, and T. J. Smayda (1987) Short-term changes in the biology of a Gulf Stream warm-core ring: phytoplankton biomass and productivity. Limnol. Oceanogr., 32, 919-929.

Holm-Hansen O., C. J. Lorenzen, R. W. Holmes and J. D. H. Strickland (1965) Fluorometric determination of chlorophyll. J. Cons. Int. Explor. Mer, 30, 3-15.

Kirk J. T. 0. (1983) Light and photosynthesis in aquatic ecosystems. Cambridge University Press, New York. 401 pp.

Lohrenz S. E., D. A. Wiesenburg, I. P. DePalma, K. A. Johnson, and D. R. Gustafson, Jr. (1988) Interrelationships among primary production, chlorophyll and environmental conditions in frontal regions of the western Mediterranean Sea. Deep-Sea Res., 35, 793-810.

Lohrenz, S. E., D. A. Wiesenburg, C. R. Rein, R. A. Amone, C. D. Taylor, G. A. Knauer, and A. H. Knap (1991) A comparison of in situ and simulated in situ methods for estimating oceanic primary production. J. Plank. Res. 14, in press.

Nelson D. M. and others (1985) Distribution and composition of biogenic particulate matter in a Gulf Stream warm-core ring. Deep-Sea Res., 32, 1347-1369.

Olson, D. B. (1990) BIOSYNOP: Biophysical studies of Gulf Stream meanders. Synoptician, 1 (3), 1-3.

Platt, T., C. L. Gallegos, and W. G. Harrison (1980) Photoinhibition of photosynthesis in natural assemblages of marine phytoplankton. J. Mar. Res., 38, 687-701.

Prieur L. and S. Sathyendranath (1981) An optical classification of coastal and oceanic waters based on the specific absorption curves of phytoplankton pigments, dissolved organic matter, and other particulate materials. Limnol. Oceanogr., 26, 671-690.

The Ring Group (1981) Gulf Stream cold-core rings: their physics, chemistry, and biology. Science, 212, 1091-1100.

Sathyendranath S. and T. Platt (1988) The spectral irradiance field at the surface and in the interior of the ocean: a model for applications in oceanography and remote sensing. J. Geophys. Res., 93, 9270-9280.

Smith R. C. and K. S. Baker (1985) Spatial and temporal patterns in pigment biomass in Gulf Stream warm-core ring 82B and its environs. J. Geophys. Res., 90, 8859-8870.

Whitledge, T. E., S. C. Malloy, C. J. Patton and C. D. Wirick. 1981. Automated nutrient analysis in seawater. Formal Report 51398, Brookhaven National Laboratory, Upton, New York, 216 pp.

Yentsch, C. S. (1974) The influence of geostrophy on primary production. Tethys, 6, 111-118.

Yoder J. A., L. P. Atkinson, S. S. Bishop, J. O. Blanton, T. N. Lee, and L. J. Pietrafesa (1985) Phytoplankton dynamics within Gulf Stream intrusions on the southeastern Unites States continental shelf during summer 1981. Cont. Shelf Res., 4, 611-635.

How Good is the Mooring Motion Correction? Tests using the Central Array Current Meter Data

Meghan Cronin, URI

Because the energetics analysis involve derivatives of the means and covariances of the temperature and velocity fields, it is important that these measurements be as accurate as possible. The questions then arises, how much error is introduced by 'correcting' the measurements to fixed horizons? Although in general, the drag on the moorings caused vertical excursions of only 50m, there were several vertical excursions of 100m on a few of the moorings. The largest excursion was nearly 500m on one mooring. Such excursions, obviously will cause significant error in the mean and covariance terms unless properly corrected.

Nelson Hogg's 1991 mooring correction scheme was used to correct the Central and Eastern moored velocity and temperature data to constant horizons. Extensive tests of this method have show that Hogg's (1991) correction scheme is very robust. The tests on the Central Array data, in particular on the M13 mooring data, are discussed here.

Hogg's (1991) method assumes that the isotherms are parallel in a temperature cross-section. This is equivalent to assuming that the vertical temperature profile has a 'canonical shape' at all times and locations. In the Gulf Stream, this assumption is not true for the warm (T > 12°C), upper water column (z < 400m) water. Because the Central Array moorings were designed to have their top current meters at approximately 330m when there was no drag on the mooring, the assumption of parallel isotherms for the entire region is tenable. Therefore, two canonical profiles (a northern and a southern) were used to correct the respective northern and southern Central Array data. Mooring M13 was on average south of the north wall and therefore uses the southern profile.

In the ideal case, there are three working current meters at mean depths of (for example) 350m, 650m, and 950m that must be interpolated (or extrapolated) to the fixed horizons at 400m, 700m, and 1000m. Two tests are shown. In the first test, the level 1 and level 3 current meters are used to interpolate 300m to level 2. The simulated level 2 current meter temperature and velocity data is then compared to the measured level 2 current meter. Figure 1a shows this comparison. The temperature error is, .7°C and the velocity errors are on the order of .06 m/s in each component. As shown in Figure 1b, the covariances of the simulated data match the measured level 2 covariances quite well. The errors are tabulated in Table 1.

Test #	1	2
err(T)	.73	.35
err(u)	.07	.15
err(v)	.05	.06
err(u'u')	.06	.27
err(v'v')	.03	.09
err(u'v')	.02	.11
err(v'T)	.23	.53

Table 1: Root-mean-square error between measured data and simulated data for test 1 and 2. Test 1 uses current meters at level 1 and 3 to interpolate to level 2. Test 2 uses current meters at level 2 and 3 to extrapolate to level 1. Units of velocity are m s^{-1}. Temperature units are °C.

Most levels need to be corrected by only 30-50m (eg. from 660m to 700m) instead of 300m. However, this test was an interpolation. A much harder test would involve an extrapolation. Therefore in the second test, we used level 2 and level 3 to extrapolate 300m to level 1. Figure 2a and 2b show the comparison between the measured level 1 data and the simulated level 1 data. The temperature error for test two was .4°C. This error is less than temperature error for test 1 because for much of the time, the top current meter was in 18°C where there is very little variability. The error in the velocity in higher for this more difficult test. As shown in Table 1, the error in u is .15 m/s and the error in v is .10 m/s. In general the simulated covariances follow the highs and lows in the measured covariances, though some peaks are greatly overestimated.
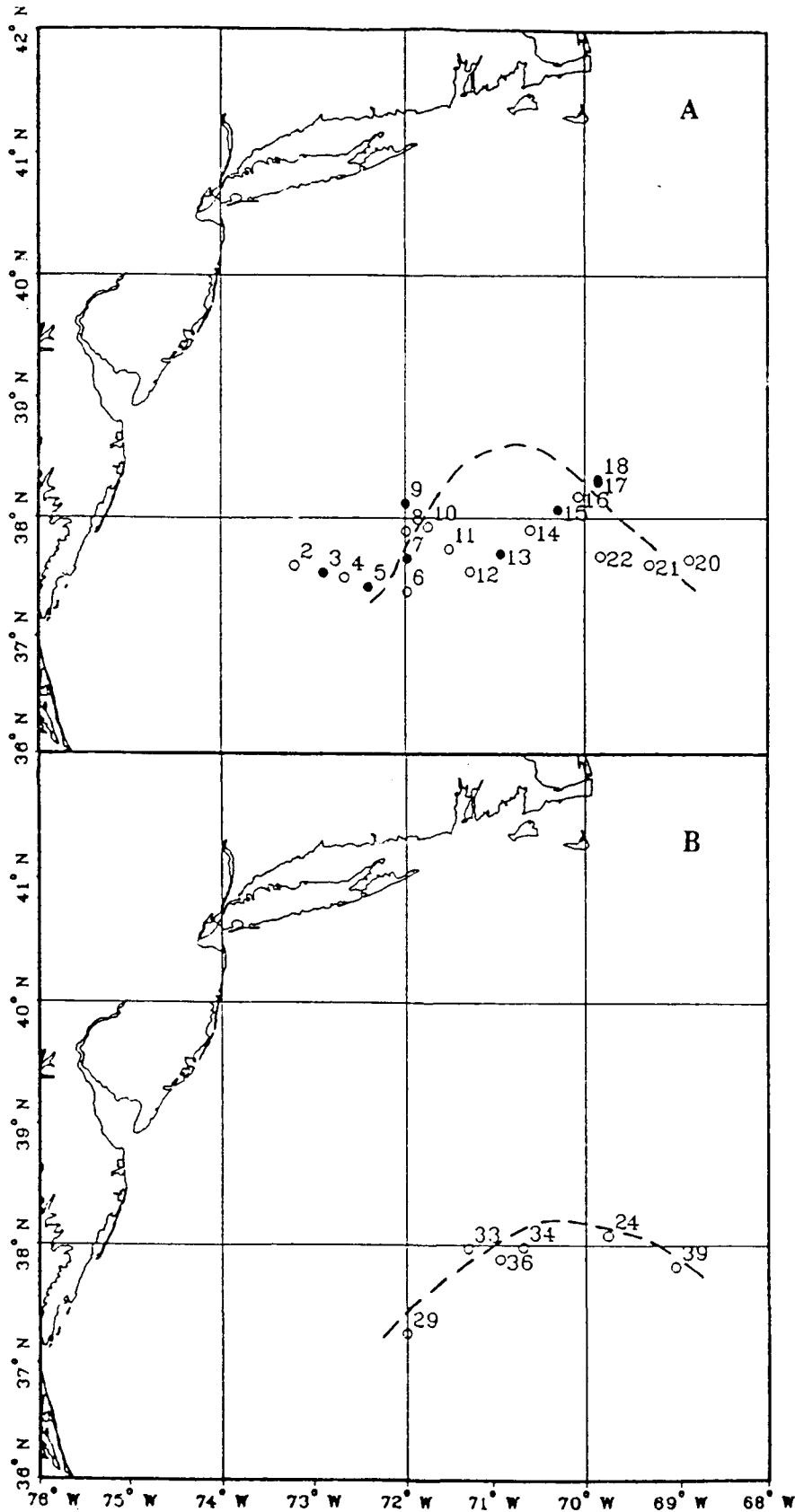
Fig 1. Location of vertical stations sampled by the R/V Cape Hatteras during 21 September through 4 October 1988. Dotted line shows location of the north wall of Gulf Stream defined by the intersection of the 12°C isotherm at 300 m. CTD and fluorometer profiles were conducted at all stations. Pigment and nutrient measurements were made at stations identified by open circles. Production measurements were made at Stations 2, 6, 10, 11, 16 20, 22, 24, 29, 33, 34, 36 and 39. A. mesoscale survey; B. additional sampling locations.
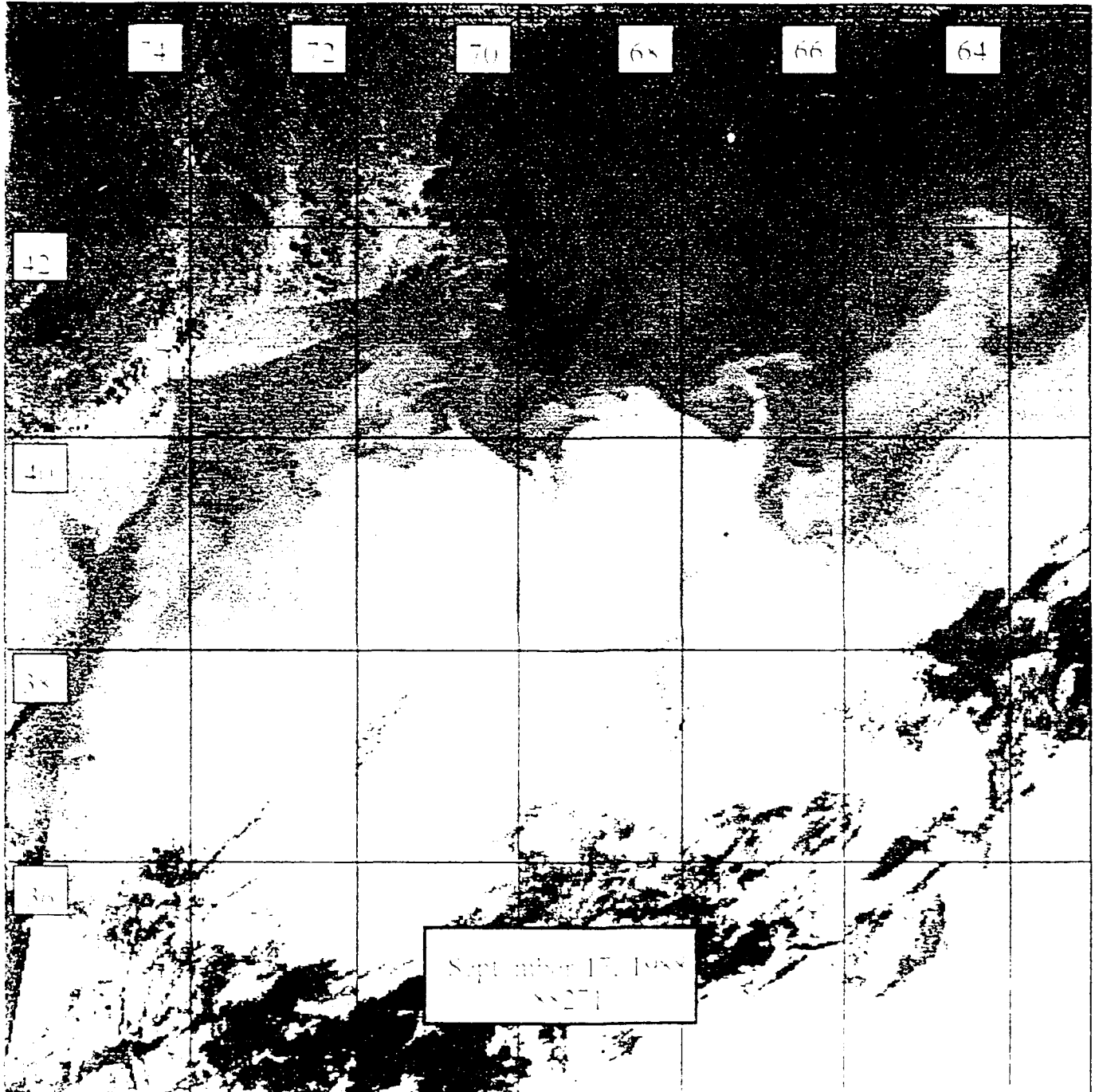
Figure 2
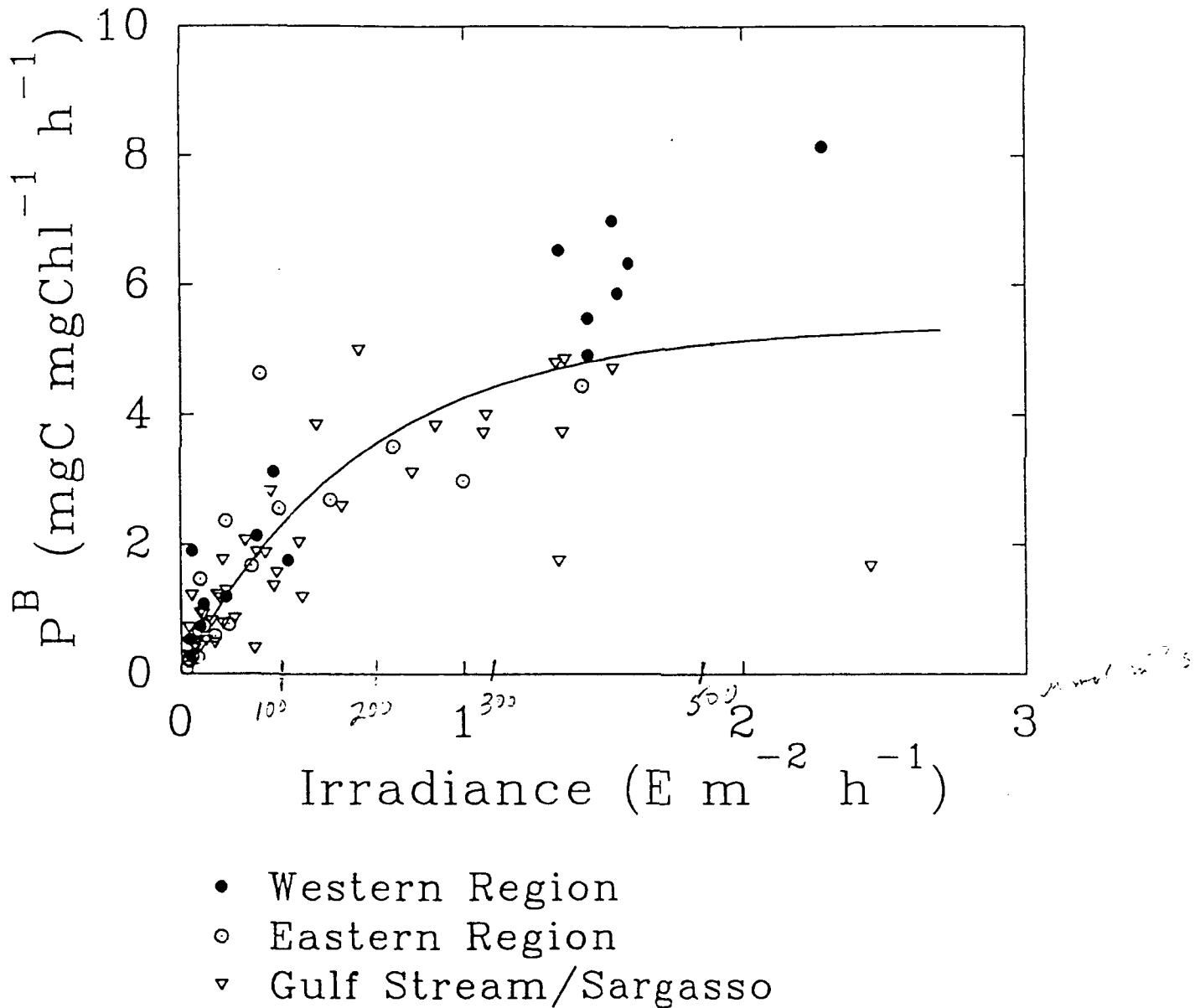
Fig 3. Chlorophyll-specific photosynthesis rates versus quantum scalar irradiance for data collected from productivity stations. Data from different regions within the meander are compared. Solid line represents nonlinear least squares fit of data to Eq. 1. Parameters and standard errors were P_s = 5.4 (0.47) mg C mg chl^{-1} h^{-1} and α = 8.4 (1.1) mg C mg chl^{-1} (E m^{-2})$^{-1}$; N = 75.
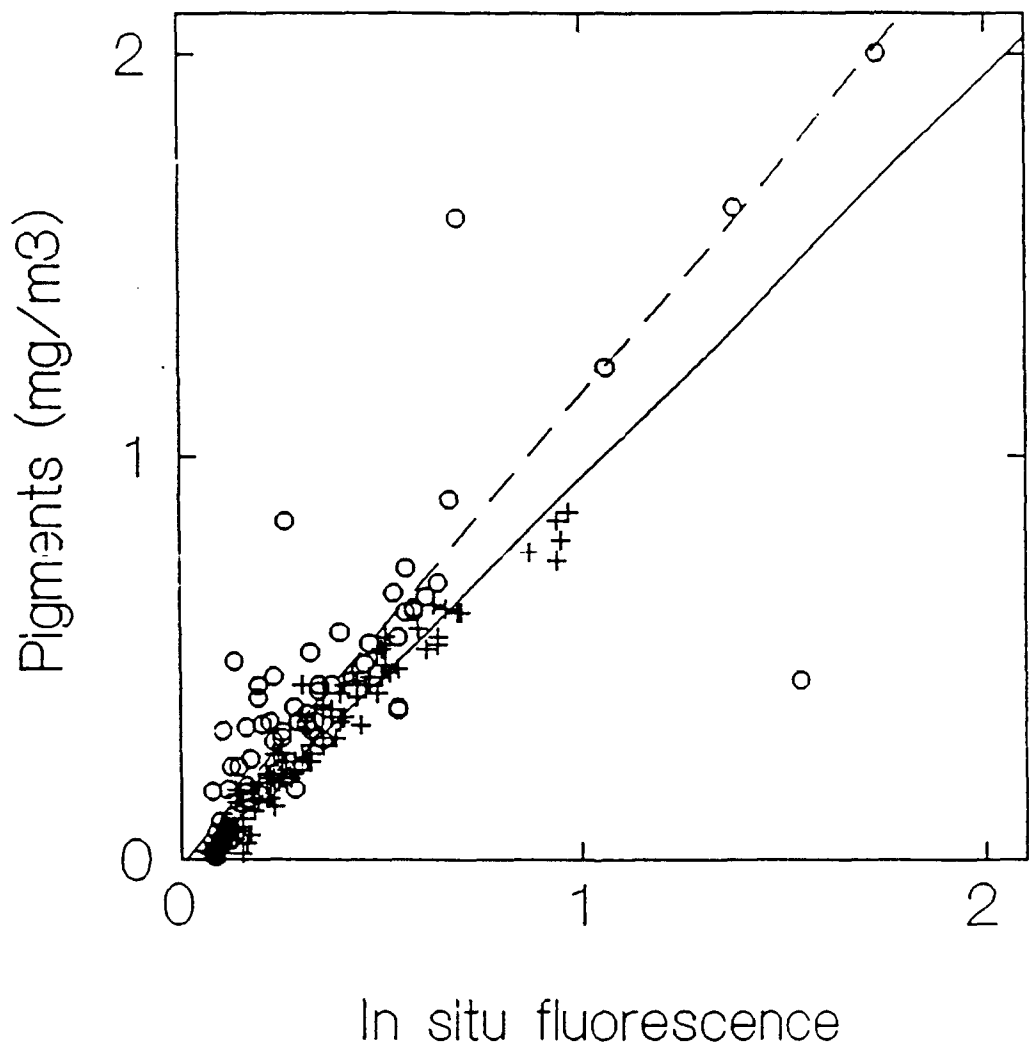
Fig 4. Comparison of *in situ* fluorescence versus measured pigment concentrations for Leg 1 (open circles) and Leg 2 (crosses). Model II regression relationships were not significantly different (dotted line, Leg 1; solid line, Leg 2).
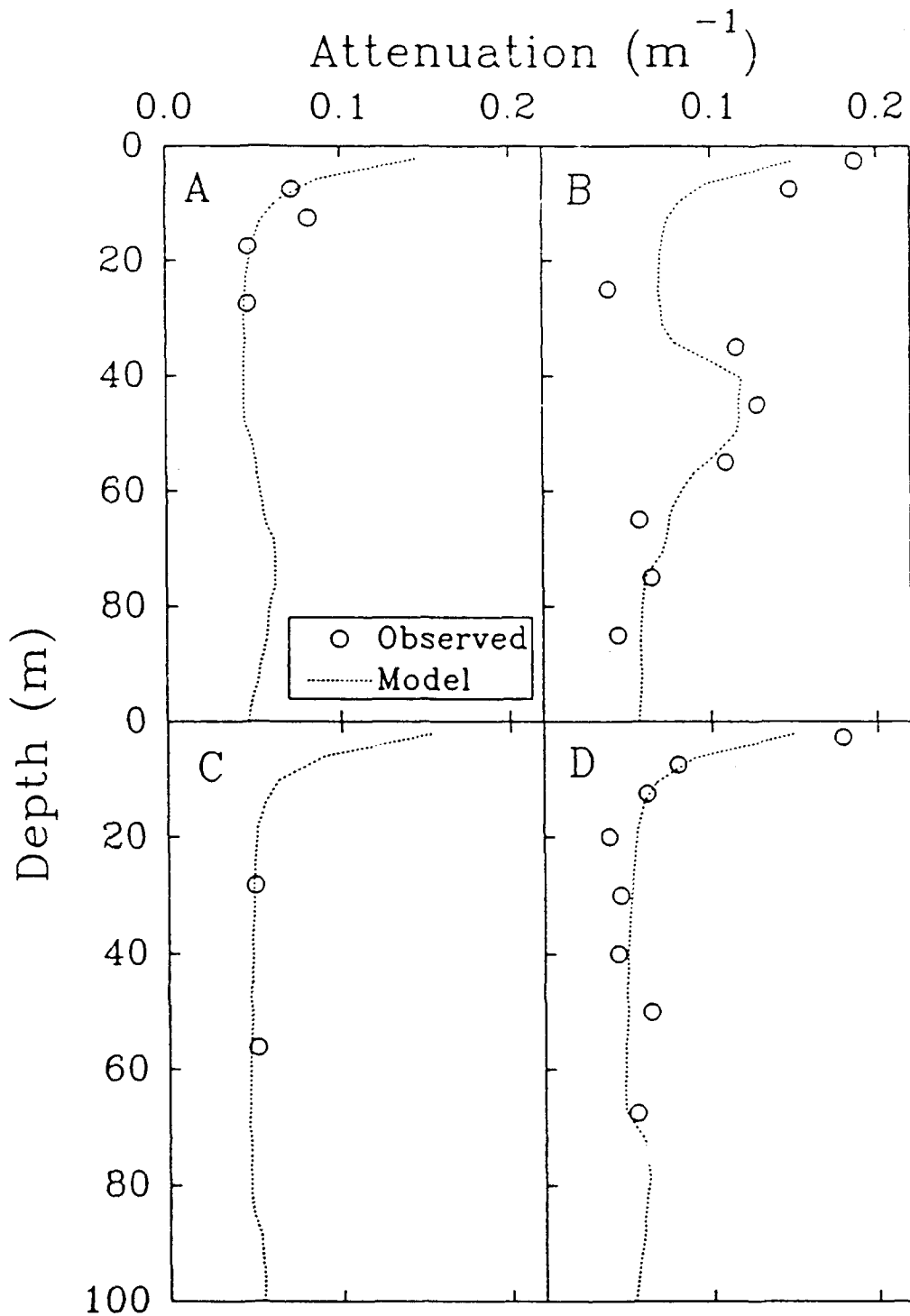
Fig 5. Comparison of measured (open circles) profiles of the vertical attenuation coefficient (KPAR) with profiles estimated (dotted line) using the spectral irradiance attenuation model.
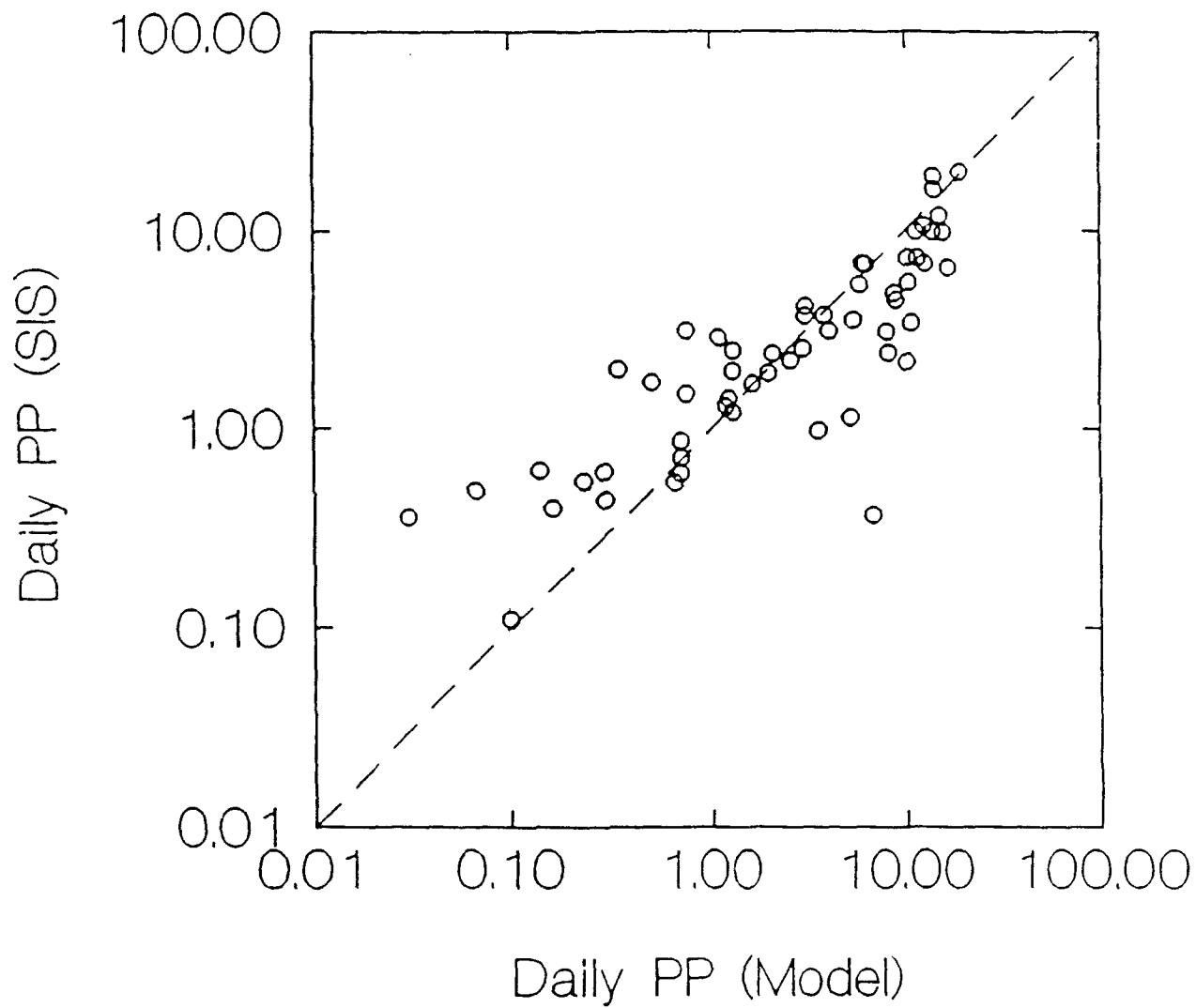
17

Fig 6. A. Comparison of modeled daily production (mg C m^{-3} d^{-1}) with estimates from 24 h simulated *in situ* (SIS) incubations (r^2=0.70; N=57; P=0.000). Line represents the 1:1 relationship.
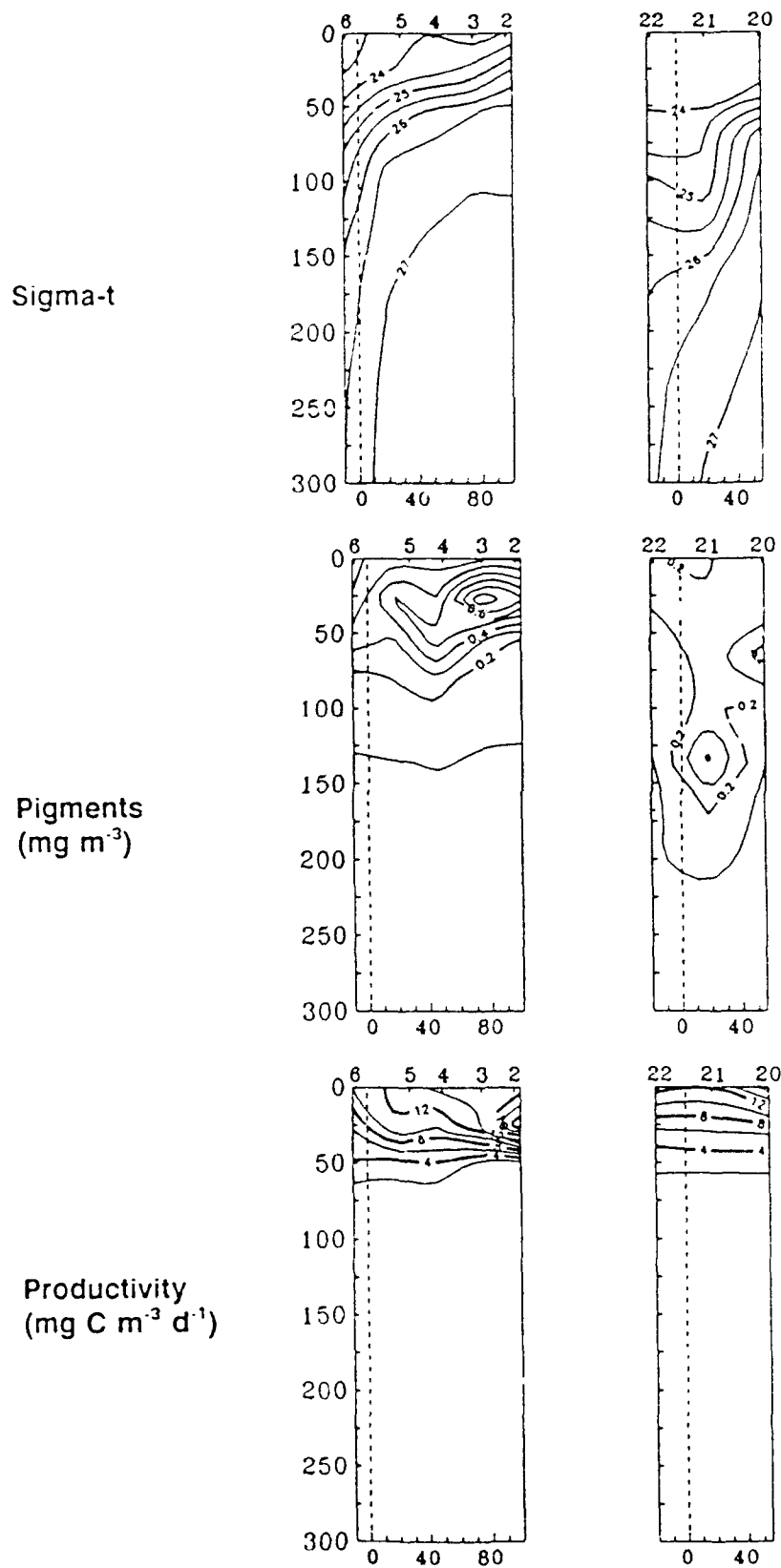
Fig 7. Σ-t, pigments, and modeled daily production for sections across the core of the Gulf Stream. Station numbers are shown along the top. Distances at the bottom are those corresponding to a curvilinear coordinate system. The cross-stream coordinate shown at the bottom is km. The nominal cross-stream coordinate of the high velocity core is O km and the north wall is usually between 25 and 20 km.